A two-dimensional amplitude study of true-amplitude time-migration and time-remigration – 2.5-D synthetic examples

Carlos A. S. Ferreira – ANP/RJ; currently at ANM/MT (Brazil)
Karina Palheta Gomes – UFAC/AC (Brazil)
Lazili Charef Eddine – ENAGEO/SONATRACH (Algeria)
Alexandre de S. Oliveira – ON/MCTI (Brazil)

Copyright 2023, SBGf - Sociedade Brasileira de Geofísica

This paper was prepared for presentation during the 18th International Congress of the Brazilian Geophysical Society held in Rio de Janeiro, Brazil, 16-19 October 2023.

Contents of this paper were reviewed by the Technical Committee of the 18th International Congress of the Brazilian Geophysical Society and do not necessarily represent any position of the SBGf, its officers or members. Electronic reproduction or storage of any part of this paper for commercial purposes without the written consent of the Brazilian Geophysical Society is prohibited.

Abstract

In this synthetic study we report on (automatically picked) true-amplitude comparisons after time-migration and time-remigration (Tygel et al., 1996; and Oliveira et al., 2023, this issue). Since the examples considered are synthetic, emphasis is put on the (generally disregarded) dimensional aspects of the amplitudes that are modeled to simulate (compressional only) seismic data when using a Kirchhoff approximation. By bearing in mind in this work that theoretical amplitudes work as “densities”, we show that when comparisons of true-amplitude weighted diffraction-stack time-migration and weighted isochrone-stack time-remigration are performed, in order to “correct” the dimensions involved certain multiplicative physical constants must come into play and that must be effectively dealt with for plotting reasons.

Introduction

Seismic reflection amplitudes are one of the most important parameters to be considered in data processing since, besides resolution, it may contain fluid information (mainly gas content) usually considered in amplitude-versus-offset (AVO) studies. Classically, it has been documented that it is affected by a sort of factors (Sheriff, 1975), including source strength, directivity, coupling, multiples, spherical divergence, etc. But since according to O’Doherty and Anstey (1971), “*modern seismic recording instruments allow precise measurements of the amplitude of reflected signals, intuitively it is expected that this amplitude information could be used to increase our knowledge of the physical properties of the reflecting Earth*”. In this sense, along the years seismic migration (either in depth or in time) has been developed as true-amplitude in order to assess measures of angle-dependent reflection coefficents of seismic data picked along key reflectors. This allows one to define an approximated image of the subsurface geology as well as assess its physical properties in an inversion procedure, like vector-weighted diffraction stack (Tygel et al., 1993).

In this expanded paper, we report on the comparison of (semi automatically) picked amplitudes along synthetic reflectors derived from (Kirchhoff) time-migration and time-remigration following the methodology presented in Oliveira et al. (2023) (this issue) for true-amplitude imaging in the time domain. In this study, due to the nature of definition for amplitudes, reflection coefficients and transmission losses factors, we investigate the “density” nature of modeled seismic reflections. This is because when modeling synthetic seismic data in 2-D or in 2.5-D, one has to notice that amplitudes in these domains are types of “densities” derived from a 3-D amplitude of a 3-D source. In this sense, square root of out-of-plane factors come into play and must adequately be included (or multiplied to), e.g., in the part of the total amplitude that contains the geometric spreading factors.

When true-amplitude imaging is considered (Hubral et al., 1996; Tygel et al., 1996), weights are to be applied in migration or demigration procedures in order to grant the best possible amplitudes between one process and another. This is the raytracing-based general approach of reflection imaging proposed by Hubral, Tygel and Schleicher in the 90s (see References). Specifically, in remigration and configuration transforms, a cascading of migration/demigration weight-functions are applied in succession in order to grant a diffraction- or isochrone-stack solution (Tygel et al., 1996). Martins (2001) reduced this general approach of Tygel et al. (1996) to the 2.5-D geometry for a single-stack solution and specified the weight-functions to be used in this domain. In Oliveira et al. (2023, this issue) migration and remigration are performed in the time-domain using weights also in time, but only the kinematic aspects were considered and their respective imaging results. Our aim here is to consider the dynamic aspect of this theory in the time domain and focus on amplitudes.

In 2.5-D raytracing, out-of-plane factors naturally are incorporated in amplitudes due to the solutions of the *ray equations* (Bleistein, 1986). But in reducing a two-fold integral to a one-fold in the high-frequency approximation using the method of stationary phase, the reciprocal of the square root of another well-known out-of-plane factor is also incorporated in amplitudes – i.e., more specifically, in the geometric spreading factor. Therefore, in synthetic modeling, beyond reflection coefficients and amplitude losses due to transmission (which are dimensionless quantities), there appears an “amplitude density” factor with dimension of $[s^{1/2}/m^2]$ (*s* for time and *m* for meters). After stack integration along each possible reflector by means of a multiplication by a differential *dx*, the result is that seismic data is dimensionally equivalent to some “*value* X *something”* (in which “something” has dimension $[s^{1/2}/m]$), which is still a “density” value. This is the starting point for the following considerations in this work. For

migration and remigration in the time domain – each process performed in their specific sequence –, their respective weight-functions are scalable, each one with a proper own dimension, and multiplied by another differential *dx*. So far (and for plotting purposes only), nothing new or wrong is performed that is unknown, such that kinematically all output sections (seismic and migrated) are correct. But if one picks several or some amplitudes along one specific reflector and tries to compare them, it will be noticed that their values are proportional but not with the same magnitude. Thus, our claim is that for a fair comparison, some sort of dimensional factors must multiply each picked amplitude in order to equalize their magnitudes and label the term "true-amplitude" in an amenable way.

It is important to state that we mean no milestone in amplitude studies with the results and proofs shown in this work. Our only intention was to clarify and understand common perceptions in seismic modeling and migration studies, to which we hope to have contributed somehow in a very ad hoc manner. We are aware that scaling factors are part of modeling, either physical or numerical.

In this work we will show the results of semi-automatic amplitude picking comparisons recovered from two 2.5-D synthetic seismic datasets (simple and complex) and discuss their physical interpretation and possible applications.

Method

Due to the nature of the 2.5-D theory, we simplify some definitions and state that 3-D sources in our examples present no issues regarding directivity or coupling. Also, attenuating properties of the medium are not included. Only geometrical spreading and reflection coefficients are concerned, this latter faking an impedance contrast that, in some sense, may be taken as optional, since reflections are the result of an analytic integration along mathematical reflectors, and may even be set to unity, when referred. Therefore, in principle picked amplitudes will be proportional to angle-dependent reflection coefficients.

In the following we consider the dimensional contributions of each numerical operation in the time domain, in sequence: modeling, weighted Kirchhoff migration, unity-weight Kirchhoff migration and Kirchhoff remigration. Each mathematical operation is responsible for a dimensional contribution to amplitude values, according to the table below:

Table 1 – Numerical contribution to amplitudes.

Numerical operation	Contribution (dimension)	Amplitude ("density")	Scaling factor
Modeling	$\frac{\sqrt{2}}{2}\frac{s^{\frac{1}{2}}}{m^2}(dx)$	$\frac{\sqrt{2}}{2}\frac{s^{1/2}}{m}$	$\sqrt{2}\frac{dx}{s^{1/2}}$
Weighted Kirchhoff	$\frac{\sqrt{2}}{2}\frac{s^{\frac{1}{2}}}{m}s^{\frac{1}{2}}(\frac{dx}{m})$	$\frac{\sqrt{2}}{2}\frac{s}{m}$	$\sqrt{2}\frac{dx}{s}$
Unity Kirchhoff	$\frac{\sqrt{2}}{2}\frac{s^{\frac{1}{2}}}{m}(\frac{dx}{m})$	$\frac{\sqrt{2}}{2}\frac{s^{1/2}}{m}$	$\sqrt{2}\frac{dx}{s^{1/2}}$
Remigration	$\frac{\sqrt{2}}{2}\frac{s}{m}\frac{s^{\frac{1}{2}}}{m^{\frac{3}{2}}}\frac{\sqrt{2}}{2}(dx)$	$\frac{1}{2}\frac{s^{3/2}}{m^{3/2}}$	$2\frac{dx^{5/2}}{s^{3/2}}$

Each entry in **Table 1** in the column "Contribution (dimension)" represents one contribution to each amplitude "density", considering the multiplication of the weight-functions of each mathematical operation by the differential *dx* of each of the numerical operations, either modeling, migration or remigration. Therefore, each result is listed in the column "Amplitude ("density")" that is inserted in each final time-migrated or remigrated seismic section. The scaling factors derived for each example are the ones that are multiplied for each picked event in the examples, turning their amplitudes dimensionless.

As described in Oliveira et al. (2023, this issue), in the examples that follows a tilde symbol ("~") over functions and variables refer to the output model, including spatial positions, time coordinates and velocities. The remaining variables and functions without tildes refer to the input model, also including spatial positions, time coordinates and velocities. The input and output model both consider an arbitrary, single fold measurement configuration of point sources and receivers distributed along the Earth surface, the location of them described by a 2-D vector parameter, $\vec{\xi} = (\xi_1, \xi_2)^T$. Vector parameter $\vec{\xi}$ varies in *A*, called migration aperture.

Therefore, for each point $(\tilde{x},\ \tilde{\tau})$ in the output, time-remigrated section simulated, the stack result $\tilde{I}(\tilde{x},\tilde{\tau})$ is obtained by a weighted stack of the input data, represented by the integral operator defined by Oliveira et al. (2023, this issue), in which $I(x,t)$ is the input, time-migrated (analytic) seismic section that is to be weighted by $K_{RM}^{(2.5D)}(x;\tilde{x},\tilde{\tau})$ and then summed up along the stacking line or inplanat $t = t_{RM}(x;\tilde{x},\tilde{\tau})$ (Tygel et al., 1996). Both functions are dependent on the point $(\tilde{x},\ \tilde{\tau})$ where the stack is to be placed, and on the variable x that specifies the location of the traces being summed in the stack. Moreover, *A* denotes the (spatial limited) aperture of the stack, the range of midpoints (in a common-offset gather) available in the time-migrated input section, $I(x,t)$. A time-reverse half-derivative is applied in order to correct the pulse shape. In 2.5D this is a counterpart to the full 3D Kirchhoff-type migration (Bleistein et al., 1987; Schleicher et al., 1993).The stacking line $t = t_{RM}(x;\tilde{x},\tilde{\tau})$ is defined by the kinematics of the operation, and the weight-function $K_{RM}^{(2.5D)}(x;\tilde{x},\tilde{\tau})$ is determined by the desired amplitude behaviour – true-amplitude and amplitude-preserving are the most common choices (Schleicher and Bagaini, 2003).

The seismic sections available to amplitude picking shall be considered in the following order: (input) seismic data (common-offset section); a diffraction-stacked (weighted) time-migrated Kirchhoff section; a unity-weight time-migrated Kirchhoff section; and a time-remigrated Kirchhoff section, in which for this latter the input section is one undermigrated, diffraction-stacked Kirchhoff section in the time domain using an inaccurate velocity model. Besides the issue of true amplitudes in time domain, we claim in the comparisons the behavior of each procedure according to the ones already described in literature.

Weight-functions

The remigration weight-function used in the examples is the product of 2.5-D migration and demigration weight-functions (Tygel et al., 1996; and Oliveira et al., 2023, this issue; Martins, 2001). Thus, in the time domain we consider, approximately:

$$K_{RM}^{(2.5D)}(x;\tilde{x},\tilde{\tau}) = \frac{\sqrt{2}}{2}\frac{\tilde{\tau}}{v_{RMS}^{3/2}}\sqrt{\frac{1}{\tilde{t}_S}+\frac{1}{\tilde{t}_G}}\left(\frac{\tilde{t}_S}{\tilde{t}_G}+\frac{\tilde{t}_G}{\tilde{t}_S}\right)\frac{1}{(t_1+t_2)}\sqrt{\frac{1}{t_1}+\frac{1}{t_2}}, \quad (1)$$

where $\tilde{t}_S$ and $\tilde{t}_G$ are double square roots (DSRs) for source and receivers in the output domain for coordinate $(\tilde{x}, \tilde{\tau})$ and $\tilde{v}_{RMS}$, while t_1 and t_2 are DSR equations in the input domain, together with v_{RMS} in this input domain. Dimensionally, this weight-function is expressed in [$s^{(1/2)}$/$meters^{(3/2)}$] units. Apart from the form of the weight-function in (1), a dimensionless stretch factor and a term regarding "local dip" at the reflector in the time domain may also be multiplied when referred. Other terms that may be multiplied in (1) are square roots of absolute values of determinants of Hessian matrices or, in 2.5-D, curvatures of diffraction traveltimes for points in the input and output domains (Tygel et al., 1998; Martins, 2001).

We do not specify the weight-functions for the weighted diffraction-stack migration because they are well known in the literature (e.g., Schleicher et al., 1993). Also, one unity weight is used for the kinematically-only Kirchhoff migration cases.

With the weights defined in this way, we will show that the remigration process "pulls" the under migrated amplitudes to the true-migrated ones, considering, of course, limitations related to aperture issues and border effects or even picking problems.

Apertures

No restrictions will be imposed to apertures. Only analytical cases are considered, using ideas of offset-continued traveltime surfaces already studied in the literature (e.g., see Fomel, 2003).

Examples

Synthetic datasets

We have tested our algorithm in two synthetic seismic datasets. A gradient of the order 0.03 Hz will be included for lateral velocity variations in the examples when referred.

Single reflector model – The first example represents a single interface of a syncline over a half-space. The velocity of the layer over the interface is set to 2.5 km/s. We have modeled a common-offset section with 2*h* = 50 m. Model parameters are Nx = 400, Nz = 200, *dx* = *dz* = 25 m, while data parameters are N_{traces} = 300, *dt* = 8 msec, where trace spacing equals to *dx* specified above, as well as source and geophone intervals. **Figure 1** depicts the modeled seismic section together with the typical bowtie pattern of reflections associated with this kind of model. The time skewing present in this input section is the result of the velocity gradient cited above. For the constant velocity example, the input section is the same, but with no skewing as seen from 4.0 km to 7.5 km in **Figure 1**.

Presalt model – Our second synthetic example considers the previously model studied in Oliveira and Ferreira (2009), which describes the results of the modeling of a simple 2-D seismic dataset acquired over a representative presalt model derived from any of the Brazilian East margin offshore basins (**Figure 2**). The geological model that was constructed to simulate the seismic section seen in **Figure 2** with its respective interval velocities is originally made of four sequences: (I) the basement (6.5 km/s); (II) the presalt section (4.5 km/s); (III) the salt layer (5.5 km/s); (IV) the Tertiary-Upper Cretaceous section, with a constant velocity gradient *v*(*z*). For the example used in this work, this model was updated to include lateral velocity variations in the Cretaceous section and in the sag/rift section and transformed to the time domain (not depicted here).

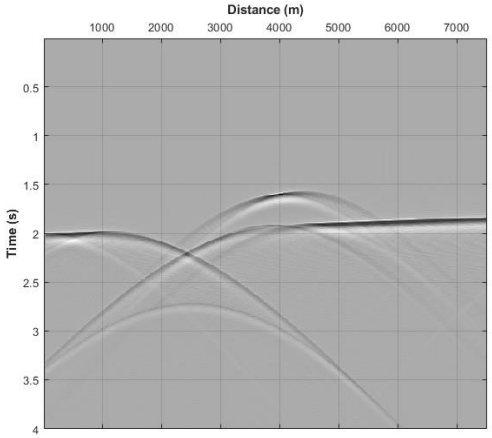

Figura 1 - Synthetic (input) common-offset seismic data (2*h* = 25 m). In the data above a velocity gradient of 0.03 Hz is considered. In the constant velocity example, the bowtie pattern is the same as depicted above, except for the time skewing due to the presence of the velocity gradient.

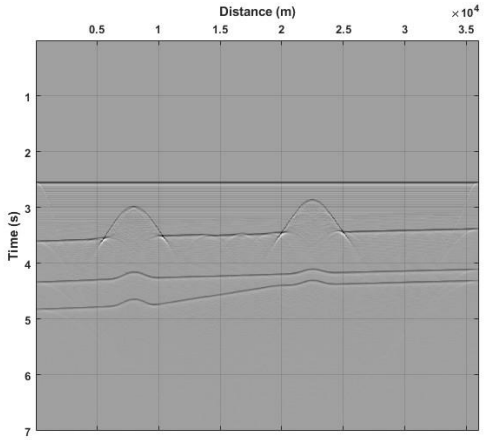

Figure 2 – Presalt model. Common-offset section (2*h* = 50 meters) simulating a 2-D seismic marine acquisition over the area of the velocity model defined in Oliveira and Ferreira (2009).

In figures **3** and **4** the results of Kirchhoff time-migrated are seen for the examples of figures **1** and **2**, respectively. Both output sections were previously weighted and migrated accordingly. The results for unity-weight and time-remigration are not depicted since they are essentially the same in terms of structures imaged. Also, the undermigrated time section is not depicted since only the

amplitude present in the remigrated results are of importance in the comparisons that will be shown in the next subsections.

Amplitude picking and comparison

In each example, a peak of a reflected and migrated event will be semi-automatically chosen in order to compare its value with the one peak in the input seismic section and in the time-migrated and time-remigrated output sections. These amplitudes will then be scaled accordingly to their "density" nature in the manner assessed in this paper and listed in **Table 1**.

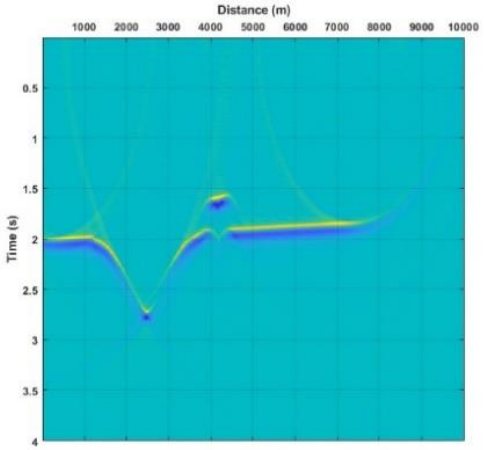

Figure 3 – Time-migrated seismic section of the input data seen in **Figure 1,** with a velocity gradient included**.** One constant velocity result of the same section was obtained (not depicted here), in which there is no time skewing.

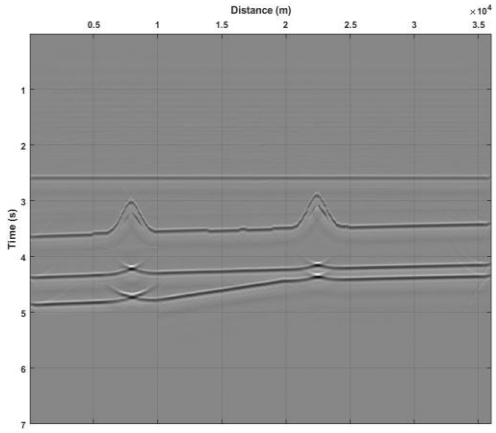

Figure 4 – Kirchhoff time-migrated seismic section of the input data seen in **Figure 2** (presalt model). Weighted time-migration here presents non-collapsed pull-ups below salt dome events and time skewing due to lateral velocity gradient.

It must be noticed that peak amplitudes are selected in order to preserve the ideia of higher value. Another possible idea is to use the envelope of the analytical signal, since this is an attribute that is related to the maximum reflection and normally preserves the lateral continuity of seismic events. Also, there may appear, in some cases, issues related to change of polarity, a feature that must be adequately cared and carefully considered. A manual picking, in these cases, may be able to resume this kind of difficult.

Results

Constant velocity model – single interface

In this example, the velocity is considered constant (2.5 km/s) above a single reflector interface. The input data is similar to the one depicted in **Figure 1** and its time-migrated output section is similar to the one depicted in **Figure 3**, but with no time skewing.

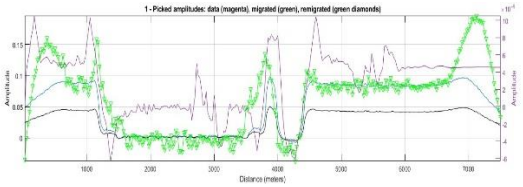

Figure 5 – Semi-automatically picked amplitudes for an event at *t* = 2 *secs* for the example of constant velocity. See text for details.

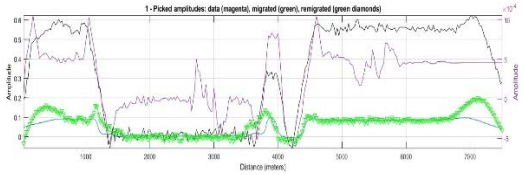

Figure 6 – Another comparison, as in **Figure 5**, but this time the black curve shows the values of the undermigrated result when compared to the other true-amplitude ones.

Figure 5 shows four amplitude profiles picked along the midpoints in figures 1 and 3 and along the unity-weight and time-remigrated Kirchhoff sections (not shown) for a continuous reflection with peak at *t* = 2 *secs*. The plot has two vertical scales, to emphasize the fact that the order of magnitudes of the amplitudes in each group of profiles are quite different. The scale of amplitudes on the right refers only to the values of modeling (magenta color), while the scale on the left include the amplitudes of unit-weight Kirchhoff time-migration (black color), true-amplitude weighted Kirchhoff migration (blue color), and Kirchhoff time-remigrated (green diamonds), respectively.

The scaling factors used in each plot are the ones listed in **Table 1**, in which they are simply multiplied to each picked event along the midpoints. It must be noticed that the values of amplitudes are proportional and scalable, as initially claimed. The situation is more clear when a laterally continuous range of values are equal in magnitude. This feature, in the example above, is fair and clearly visible along midpoints 5.0 to 7.0 km. Also, it is clear that the order of magnitude of the modeled amplitudes is much smaller than the ones time-migrated and time-remigrated, when their respective weight-functions are used. Weighted Kirchhoff migration corrects amplitudes from geometrical spreading, therefore it presents higher values in relation to the migration with unitary weight. As for the time-

remigrated amplitudes they are practically the same as the weighted Kirchhoff result. In the general approach to seismic imaging of Hubral, Tygel and Schleicher, the cascading of a migration/demigration or a single stack solution grants the best possible amplitudes in a preserving way. For this constant-velocity (and simple) example, this is a faithful statement of this fact.

A final interesting comparison for the constant velocity example is shown in **Figure 6**. This time, the black curve of amplitudes along midpoints depicts the picked values of the undermigrated Kirchhoff result, showing that these values of amplitudes are much even higher or overestimated than the weighted Kirchhoff result, and therefore its amplitudes are not the best possible ones. When this data is time-remigrated, following the lines of Oliveira et al. (2023, this issue), the output amplitudes are true again, as predicted in theory (Hubral et al., 1996; Tygel et al., 1996). This again shows that time-remigration "pulls" undermigrated amplitudes to their best true-amplitude results.

Lateral velocity variation – single interface

When lateral velocity variation is present, time-skewing is one of the features commonly present in time-migration (Black and Brzostowski, 1994; Bevc et al., 1995). **Figure 3** is already a skewed version of the input seismic section for the constant velocity case. Again, **Figure 7** depicts the comparison of picked amplitudes, for the same event at *t* = 2 *secs,* in the same manner as in **Figure 5**. This time the automatic picking for this temporal sample will vary along midpoints, including even polarity changes due to skewing. This is an example in which a manual picking should come into play, in order to preserve the lateral continuation of the events picked.

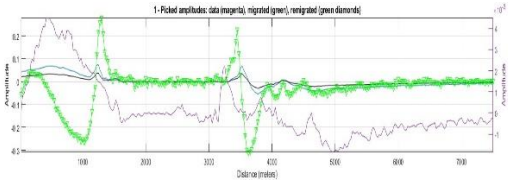

Figure 7 - Semi-automatically picked amplitudes for an event at *t* = 2 *secs* for the example of lateral velocity variation. See text for details.

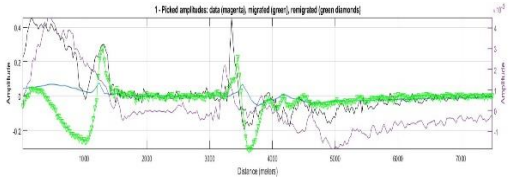

Figure 8 - Another comparison, as in **Figure 6**, but this time the black curve shows the values of the undermigrated result when compared to the other true-amplitude ones.

Figure 8 just depicts the same behavior of amplitudes when the true-amplitude results are compared to the undermigrated ones. Again, time-remigration "pulls" undermigrated amplitudes to their best true-amplitude results.

Once again we call attention to the fact that in this latter example, amplitudes were automatically picked, whereas it should have been manually done. But even with the presence of this picking problem, we observe that physically the results are conclusive, agreeing with the one in the constant velocity example.

Presalt model

For this synthetic model of the Brazilian presalt, we have to consider, particularly, that the 2.5-D amplitudes were modeled with amplitudes "densities" with dimension $1/(\sqrt{2}m^{\frac{3}{2}})$. Therefore, amplitudes are scaled with $\sqrt{2}dx^{1/2}$. **Table 2** summarizes all quantities involved.

Table 2 – Presalt model contribution to amplitudes.

Numerical operation	Contribution (dimension)	Amplitude ("density")	Scaling factor
Modeling	$\frac{1}{\sqrt{2}m^{3/2}}(dx)$	$\frac{1}{\sqrt{2}m^{1/2}}$	$\sqrt{2}dx^{1/2}$
Weighted Kirchhoff	$\frac{1}{\sqrt{2}m^{1/2}}\frac{\sqrt{2}}{2}s^{\frac{1}{2}}(\frac{dx}{m})$	$\frac{1}{2}\frac{s^{1/2}}{m^{1/2}}$	$2\frac{dx^{1/2}}{s^{1/2}}$
Unity Kirchhoff	$\frac{1}{\sqrt{2}m^{1/2}}(\frac{dx}{m})$	$\frac{1}{\sqrt{2}m^{1/2}}$	$\sqrt{2}dx^{1/2}$
Remigration	$\frac{1}{2}\frac{s^{1/2}}{m^{1/2}}\frac{s^{\frac{1}{2}}}{m^{\frac{3}{2}}}\frac{\sqrt{2}}{2}(dx)$	$\frac{\sqrt{2}}{4}\frac{s}{m}$	$2\sqrt{2}\frac{dx}{s}$

The picking procedure for this example is the most challenging one. There are several issues of processing related to this model. The presence of aliasing noise in modeling and migration seems to contaminate the automatic sample picking in the straightforward manner in which our procedures have been done in the previous examples. Our opinion, without proving here, is that a careful manual picking should be mandatory in order to compare all amplitudes, time-migrated or time-remigrated, in a fair way. But since manual picking was not available to us during the writing of this paper, the only solution was to band-pass the data in each of the procedures so as to eliminate as much noise as possible. Therefore, an Ormsby band-pass filter was applied to the input seismic data before kinematic and weighted migrations, as well as to the undermigrated data before the time-remigration procedure. In terms of kinematic imaging, these filtering proved to be quite satisfactory.

Due to these problems, we have chosen two specific time samples (**Figure 9**) of the model in order to compare the values of picked amplitudes along the migrated and remigrated sections. These samples are very close to each other in time and are representative of the top of the salt layer of the geological model. Since the picked events are referred to a single sample in time, the lateral variation along midpoints shall not follow a continuous trend, but sometimes even oscillate between positive and negative values (change of polarity). Notice that in the areas of the two salt domes (in the ranges 5 km – 10 km and 20 km – 25 km, respectively) the picked values must be disregarded, since there are no seismic events there, just noise (see **Figure 4**). In these ranges, the picked values from the input seismic section are located between two distinctive spikes that indicate the region where edge diffractions of the salt domes occur (see **Figure 2**).

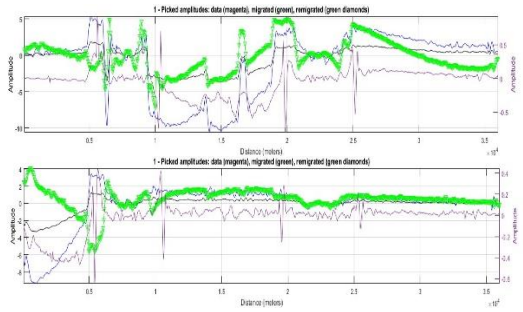

Figure 9 – Picked amplitudes for events at 3.54 *secs* and 3.64 *secs*, representative of the top of the salt layer.

As before, it must be noticed that the picked time-migrated and time-remigrated amplitudes are proportional to the ones from the input seismic data, according to their respective scales, after the use of the scaling factors listed in **Table 2**. Also, it is important to notice that, in both examples, the remigrated picked values follows closely (and proportionally) the weighted Kirchhoff values, as already shown in previous examples.

Conclusions

We have successfully studied the scaling of amplitudes derived from weighted time-migration and time-remigration processes and their comparison to scaled amplitudes picked along input seismic data.

Recognizing that numerically modeled 2.5-D data amplitudes work as “densities”, through dimensional considerations several scale factors were determined and then directly multiplied to picked amplitude values in order to equalize their magnitude and scales, when these results are compared along output sections. In this way, we have shown ad hoc that picked time-migrated and time-remigrated amplitudes, corrected for geometrical spreading, are proportional to amplitudes picked from their input seismic data.

We have tested the present procedure in two synthetic, common-offset, 2.5-D seismic data. The input data of the first model considers only an interface separating two media, where for the first layer the cases of constant velocity and initial velocity with lateral variation were accounted for. The input data for the second model is representative of a 2-D marine acquisition over a regional presalt area derived from any of the Brazilian East Margin offshore basins, including lateral velocity variations in the Cretaceous and sag/rift stratigraphic sections.

The results obtained in all examples showed that the scaling of amplitudes by dimensional factors is capable of equalizing magnitudes of the picked events, at least proportionally, increasing the confidence of its physical interpretation.

Acknowledgments

The first author would like to thank ANP/RJ and ANM/MT for the permission to take part in this work. The last author would like to thank CNPQ for his MSc scholarship, during all the stages of this research.

References

Black, J. L.; Brzostowski, M. A., 1994, Systematics of time-migration errors: *Geophysics*, **59**, 1419-1434.

Bevc, D.; Black, J. L.; Palacharla, G., 1995**.** Plumes: Response of time migration to lateral velocity variation. *Geophysics*, 60, 1118-1127.

Bleistein, N., 1986. Two-and-one-half dimensional in-plane wave propagation: *Geophysical Prospecting*, **34**, 686–703.

Bleistein, N.; Cohen, J. K.; Hagin, F. G., 1987. Two-and-one-half dimensional Born inversion with na arbitrary reference. *Geophysics*, **52**, 26-36.

Fomel, S., 2003. Velocity continuation and anatomy of residual prestack time migration. *Geophysics*, **68**, 1662-1672.

Hubral, P., Schleicher, J. & Tygel, M., 1996b. A unified approach to 3-D seismic reflection imaging-Part I: Basic concepts, *Geophysics*, **61**, 742-758.

Martins, J. L., 2001. Migração, demigração e imageamento em 2.5D com inclusão de alguns casos analíticos. Tese de doutorado (in Portuguese). Unicamp/SP, 107p.

Oliveira, A. S.; Ferreira, C. A. S., 2009. Modeling of a synthetic presalt 2D seismic dataset representative of offshore East margin basins (Brazil) – preliminary results. 11th Int. Congress of the Brazilian Geophys. Soc.

O’Doherty, R. F.; Anstey, N. A., 1971. Reflections on amplitudes. *Geophysical Prospecting*, **19**, 430-458.

Oliveira, A. S.; Lourenço, J.; Ferreira, C. A. S., 2023. Kirchhoff time-remigration and time-to-depth conversion – preliminar studies and possible applications. 18th Int. Congress of the Brazilian Geophys. Soc. Submitted.

Schleicher, J.; Tygel, M.; Hubral, P., 1993. 3D true-amplitude finite-offset migration. *Geophysics*, **58**, 1112-1126.

Schleicher, J.; Bagaini, C., 2003. Controlling Amplitudes in 2.5D common-shot migration to zero offset. Wave Inversion Technology.

Sheriff, R. E., 1975. Factors affecting seismic amplitudes. *Geophysical Prospecting*, **23**, 125-138.

Tygel, M.; Schleicher, J.; Hubral, P.; Hanitzsch, C., 1993. Multiple weights in diffraction stack migration. *Geophysics*, **59**, 1820-1830.

Tygel, M., Schleicher, 3. & Hubral, P., 1996. A unified approach to 3-D seismic reflection imaging-Part IT: Theory, *Geophysics*, **61**, 759-775.

Tygel, M.; Schleicher, J.; Hubral, P.; Santos, L. T., 1998. 2.5D true-amplitude Kirchhoff migration to zero-offset in laterally inhomogeneous media. *Geophysics*, 63, 557-573.